

High-early-strength ductile cementitious composites with characteristics of low early-age shrinkage for repair of infrastructures

Mustafa Şahmaran · Muḥannad Al-Emam ·
Gürkan Yıldırım · Yunus Emre Şimşek ·
Tahir Kemal Erdem · Mohamed Lachemi

Received: 8 July 2013 / Accepted: 12 December 2013 / Published online: 20 December 2013
© RILEM 2013

Abstract Reduced performance in concrete infrastructures is mainly caused by the formation of cracks, which may arise due to deteriorating mechanisms during service life. In most cases, reduced performance calls for urgent repairs to the degraded section. Therefore, it is highly desirable to develop dimensionally stable, ductile repair materials that can attain adequately high strength in a limited amount of time, compensate for significant deformation due to mechanical and environmental loadings, and prevent early-age shrinkage cracks. In this paper, the performance of such a material (high-early-strength engineered cementitious composites, HES-ECC, with very low early-age shrinkage capacity) was investigated by studying mechanical properties and dimensional stability. Composites were produced with different water

to cementitious materials and slag to Portland cement ratios. In order to enhance composite properties in terms of ductility and early-age shrinkage characteristics, saturated lightweight aggregates replaced sand in the mixtures. The experimental results show that the majority of HES-ECC mixtures developed in this study attained compressive strength values of more than 20.0 MPa and minimum flexural strength of 6.0 MPa within 6 h. Moreover, the HES-ECC mixtures exhibited strain-hardening behavior with strain capacities comparable to normal strength ECC, as well as substantially reduced autogenous shrinkage strain, both of which are unlikely to trigger the formation of cracks in tension at early ages. The integration of these conflicting parameters suggests that HES-ECC can easily meet the need for fast and durable repairs.

M. Şahmaran (✉)
Department of Civil Engineering, Gazi University,
Ankara, Turkey
e-mail: sahmaran@gazi.edu.tr

M. Al-Emam · G. Yıldırım · Y. E. Şimşek
Department of Civil Engineering, Gaziantep University,
Gaziantep, Turkey

T. K. Erdem
Department of Civil Engineering, Izmir Institute of
Technology, Izmir, Turkey

M. Lachemi
Department of Civil Engineering, Ryerson University,
Toronto, ON, Canada

Keywords High-early-strength engineered
cementitious composites (HES-ECC) ·
Internal curing · Mechanical properties

1 Introduction

Concrete material often cracks, and because cracking significantly damages the durability properties of concrete, it is an issue of major concern in the construction industry. Deterioration mechanisms leading to cracking in concrete may involve environmental (e.g. freeze–thaw cycles, corrosion and different shrinkage types), external (e.g. poor workmanship



and construction practices) and mechanical effects (e.g. fatigue) [1–3]. Concrete may also lose its load carrying capacity or even spall and fail with the influence of more catastrophic impacts such as earthquakes, hurricanes and fire. This reduction in performance often requires rapid and effective repair of deteriorated sections.

Increasing repair, retrofit and maintenance costs of existing concrete structures is a growing concern. In the U.S. alone, the estimated cost for maintenance of deteriorated roads and bridges over the next 20 years is a staggering \$1.8 trillion [4]. In Asia, it is \$2 trillion. In most European countries, the cost of repair already exceeds that of new construction [5]. Therefore, the design of cost-efficient, durable and high performance repair materials is extremely desirable for the sustainability of different infrastructure types such as bridge decks, highway pavements, parking structures, and airport runways.

When traffic congestion is factored into repairs, an ideal repair material needs to show high strength at early ages. The required time for a repair job is approximately 6–8 h, and construction is mostly done at night so that the road can be opened the next morning without any interruption in traffic flow. While high early compressive strength is an indispensable material property for repair materials, it also causes an increase in the elastic modulus and brittleness of the material, which can facilitate the formation of cracks. Unfortunately, repairs made with conventional materials are more prone to cracking; almost half of traditional concrete repairs fail [6]. In addition to the premature cracking of high early strength repair materials that might arise under several service conditions [7], cracks also originate due to autogenous shrinkage. Differences in thermal gradients stand as one of the problematic issues for the design of truly resilient repair materials. Therefore, to be used as a repair material, concrete must gain sufficiently high compressive strength at early ages, show adequate flexural characteristics and compensate for the drawbacks (e.g. crack formation) caused due to the effects of different shrinkage mechanisms.

Engineered cementitious composites (ECC) is a special type of high performance fiber-reinforced cementitious composite featuring high ductility and damage tolerance under mechanical loading, including tensile and shear loadings [8, 9]. By employing

micromechanics-based material optimization, tensile strain capacity in excess of 3 % under uniaxial tensile loading can be attained with only 2 % fiber content by volume [8, 10, 11]. Strain-hardening behavior, which is one of the material characteristics of ECC, is associated with the multiple tight cracking phenomenon of the brittle matrix. The formation of multiple microcracks with widths of less than 100 μm is an intrinsic material property of ECC. Multiple microcracking is realized through an increment in ductility that is considered one of the most influencing parameters for the durability of repair materials [12]. However, high early strength causes reductions in ductility due to increased paste maturity and its damaging effects on the fiber–matrix interface. In addition, increased early compressive strength may result in cracks caused due to several shrinkage types. Over the years, many researchers have concentrated on high early strength and fast-stiffening concrete materials and gathered invaluable information about how these properties were obtained [13–15]. However, only a few studies target the simultaneous attainment of sufficient compressive strength and tensile ductility at early ages [12, 16]. In those studies, high tensile ductility through multiple microcracking was effectively achieved with the introduction of artificial flaws into the matrix. Thus, a similar approach was used throughout this study in order to integrate tensile ductility and high early strength.

In this study, emphasis was placed on the design of high early strength ECC (HES-ECC), which can show characteristics superior to other repair materials currently available in the market. To do this, three mixtures with different ground granulated blast furnace slag (S) to Portland cement (PC) ratio (S/PC) and water to cementitious material ratio (W/CM) were produced. During the production of mixtures, pre-soaked expanded perlite was used as saturated lightweight aggregate (LWA). Maximum aggregate sizes (MASs) of LWA used in the mixtures were 2 and 4 mm. LWA replacement rates were 25 and 50 % by volume. The current study is unique in that pre-soaked LWAs were utilized not only as artificial flaws to tailor the ductility of the matrix, but also as internal moisture reservoirs to minimize early age cracking due to increased paste maturity. The testing program was composed of two phases. In the first phase, mechanical properties of the specimens were evaluated, and in the

second, dimensional stability was investigated. Mechanical properties including compressive strength, flexural strength, flexural deformation, uniaxial tensile strength and strain, and fracture toughness results were presented. The dimensional stability phase covered results obtained from autogenous shrinkage test.

2 Research significance

Concurrent attainment of high early strength, tensile ductility and low early-age shrinkage is a challenging aim for repair materials due to conflicting design approaches of different properties. This paper presents the performance analysis of a new repair material, HES-ECC, which combines high early strength, tensile deformability and very low early-age shrinkage characteristics. To date, there has been limited information available in the literature related to the performance of such materials. This study aims to fill that knowledge gap.

3 Experimental program

3.1 Materials and mixture proportions

As mentioned in the introduction, an ideal repair material must meet certain compressive strength values, especially at early ages. However, despite its significance in repair materials, there is no specification for minimum compressive strength in the existing standards. Several authorities suggest different minimum limits for compressive strength values, depending on the specific construction need. According to Parker and Shoemaker [17], 13.8 MPa of initial compressive strength is adequate for a repair material to be resistant against several types of deformation. The New Jersey State Department of Transportation (NJDOT) suggests 20.7 MPa of compressive strength at the age of 6 h for a “fast-track mix” developed in the mid-1990s [18]. For rapid-setting cementitious concrete, 6.9 and 20.7 MPa of compressive strength were recommended at three and 24 h, respectively, by the Federal Highway Administration [19]. In the present study, the minimum requirement for compressive strength was agreed to be at least 20 MPa at the end of 6 h.

In order to meet the specified compressive strength without sacrificing desired ECC material properties (i.e. superior tensile ductility) several trial mixtures were designed with consideration for micromechanical design constraints. As a result of the preliminary studies, three different HES-ECC mixtures with two water to cementitious material ratios (W/CM) (i.e. 0.23 and 0.34) and three slag to PC ratios (S/PC) (i.e. 0.00, 0.60 and 0.84) were selected. Because of micromechanical design constraints, the total amount of water and solid fractions were kept constant (binder+aggregate) in all mixtures. Partial replacement using slag reduces the environmental burden. Further, it has been found that incorporating high amount of slag can reduce the matrix toughness and improve the robustness of ECC in terms of tensile ductility [20]. Additionally, unhydrated particles of slag with small particle size serve as filler particles resulting in higher compactness of the fiber/matrix interface transition zone that leads to a higher frictional bonding [15]. This aids in reducing the steady-state crack width beneficial for long-term durability of the structure.

The mixture proportions for the three HES-ECC mixtures are presented in Table 1. The ingredients used in the mixtures were CEM I 52.5R high early strength PC, ground granulated blast furnace slag (S), silica sand, expanded lightweight perlite aggregate, polyvinyl-alcohol fibers (PVA), water, high range water reducing admixture (HRWRA) and accelerating admixture (AA). The physical and chemical characteristics of PC and S are presented in Table 2. In the mixtures, fine silica sand with a MAS of 400 μm was utilized, along with pre-soaked expanded fine and coarse perlite with MAS of 2.0 and 4.0 mm, respectively. Polycarboxylate ether type HRWRA with a specific gravity of 1.1 and 40 % solid content was added to the mixtures until favorable fresh mortar characteristics were visually observed. Calcium nitrate salt based accelerator with the specific gravity of 1.3 was used to accelerate the reactions between the water and cement, especially when the initial set was reached. PVA fibers with a diameter of 39.0 μm and a length of 8.0 mm were purposely manufactured with a tensile strength (1620 MPa), elastic modulus (42.8 GPa), and maximum elongation (6.0 %) matching those needed for strain-hardening performance. The surface of the PVA fibers was coated with hydrophobic oiling agent (1.2 % by weight) to reduce interfacial

Table 1 HES-ECC mixture proportions

Ingredients (kg/m ³)	HES-ECC_1						HES-ECC_2						HES-ECC_3						
	Control		C_LWA		F_LWA		Control		C_LWA		F_LWA		Control		C_LWA		F_LWA		
	25 %	50 %	25 %	50 %	25 %	50 %	25 %	50 %	25 %	50 %	25 %	50 %	25 %	50 %	25 %	50 %	25 %	50 %	
Total water	298	298	298	298	298	298	299	299	299	299	299	299	299	299	299	299	299	299	299
Portland cement	719	719	719	719	719	719	819	819	819	819	819	819	819	819	819	819	819	819	819
Slag	600	600	600	600	600	600	493	493	493	493	493	493	493	493	493	493	493	493	493
Quartz sand	587	439	293	293	439	293	598	449	300	449	300	449	300	449	300	449	300	449	300
LWA (perlite)	–	50.0	100	100	50.0	100	–	51.0	102	51.0	102	–	51.0	102	51.0	102	–	51.0	102
PVA fiber	26.0	26.0	26.0	26.0	26.0	26.0	26.0	26.0	26.0	26.0	26.0	26.0	26.0	26.0	26.0	26.0	26.0	26.0	26.0
HRWR	13.8	10.8	8.6	10	8.6	10	12.6	10.1	8.7	9.7	7.9	12.6	10.1	8.7	9.7	7.9	12.6	10.1	8.7
AA	12.3	12.3	12.3	12.3	12.3	12.3	12.3	12.3	12.3	12.3	12.3	12.3	12.3	12.3	12.3	12.3	12.3	12.3	12.3
Volumetric mass	2256	2155	2057	2154	2057	2154	2260	2158	2060	2158	2059	2260	2158	2060	2158	2059	2260	2158	2059
Total [W/(C + S)]	0.23	0.23	0.23	0.23	0.23	0.23	0.23	0.23	0.23	0.23	0.23	0.23	0.23	0.23	0.23	0.23	0.23	0.23	0.23
IC [W/(C + S)]*	–	0.08	0.17	0.08	0.15	0.15	–	0.09	0.17	0.08	0.16	–	0.09	0.17	0.08	0.16	–	0.09	0.17
Effective [W/(C + S)]	0.23	0.31	0.40	0.31	0.38	0.38	0.23	0.32	0.40	0.31	0.39	0.23	0.32	0.40	0.31	0.39	0.23	0.32	0.40
LWA/total sand	–	0.25	0.50	0.25	0.50	0.50	–	0.25	0.50	0.25	0.50	–	0.25	0.50	0.25	0.50	–	0.25	0.50
S/PC	0.84	0.84	0.84	0.84	0.84	0.84	0.60	0.60	0.60	0.60	0.60	0.60	0.60	0.60	0.60	0.60	0.60	0.60	0.60

* Internal curing (IC) water to cementitious material (CM = Cement+Slag) ratio



Table 2 Chemical and physical properties of Portland cement and slag

	PC	S
Chemical compositions		
CaO	65.7	35.1
SiO ₂	21.6	37.6
Al ₂ O ₃	4.1	10.6
Fe ₂ O ₃	0.26	0.28
MgO	1.30	7.90
SO ₃	3.30	2.90
K ₂ O	0.77	1.10
Na ₂ O	0.19	0.24
Loss on ignition	3.20	2.80
SiO ₂ +Al ₂ O ₃ +Fe ₂ O ₃	25.9	48.4
Compound compositions (Bogue's equation)		
C ₃ S	65.2	–
C ₂ S	12.2	–
C ₃ A	10.3	–
C ₄ AF	0.79	–
Physical properties		
Specific gravity	3.06	2.80
Blaine fineness (m ² /kg)	460	425

chemical bond strength between fiber and matrix with the aim of attaining strain hardening-performance [21]. The expanded coarse perlite (C) used in this study had water absorption capacity of nearly 144 % and specific gravity of 0.88, and values for the fine perlite (F) were 131 % and 0.92. The effects of saturated LWA usage on different shrinkage and mechanical properties were monitored on HES-ECC mixtures containing 25 % (C or F_25 %) and 50 % (C or F_50 %) of LWA replacements, by total aggregate volume. HES-ECC mixtures without LWAs (control) were also produced for comparison purposes. During the production of HES-ECC mixtures, a mortar mixer with a 20 l capacity was used. All the solid ingredients were mixed at 100 rpm until a homogeneous blend was obtained. Water, HRWR and AA were then added into the dry mixture. As soon as adequate plasticity was reached, the speed of the mixer was increased to 150 rpm and mixing was continued for 1 more minute, then 300 rpm for an additional 2 min to obtain a consistent and uniform ECC matrix. As the last step, PVA fibers were added into the fresh mixture at 150 rpm and mixed in for 3 more minutes.

3.2 Specimen preparation and testing

Twenty-four prismatic (360 × 75 × 50 mm), 18 coupon (200 × 75 × 12.5 mm) and 24 cubic (50 mm) specimens were produced from each HES-ECC mixture to be used in flexural, uniaxial tensile and compressive strength tests. These tests were performed at the ages of 6, 24 h, 7 and 28 days. Because of long specimen preparation period, uniaxial tensile test was not performed for 6 and 24 h. The specimens were stored in plastic bags at 95 ± 5 % RH, 23 ± 2 °C until the age of testing. Flexural parameters were measured by using four-point bending tests performed on a closed-loop controlled material test system with a loading rate of 0.005 mm/s. The flexural loading was applied from a span length of 304 mm and a central span length of 101 mm. During the flexural tests, the load and mid-span beam deflection were recorded on a computerized data recording system. The flexural deflection capacity of specimens was measured with the help of a LVDT placed on the test set-up. In the flexural stress-deformation curves, the maximum stress is defined as the flexural strength (modulus of rupture—MOR), and the corresponding deflection is defined as the flexural deformation capacity.

Direct tensile tests were conducted using a closed-loop controlled material test system under displacement control at a rate of 0.005 mm/s. Prior to testing, aluminum plates were glued to both ends of the coupon specimen to facilitate gripping. At least five measurements were done for each testing age. After 1-day curing of the glue, the specimen was fixed on the test set-up by clamping the aluminum plate-glued ends. A 100 mm gauge length of the central section of coupon specimens was marked with strips of fluorescent, white tape to enable extension to be measured continuously using a video extensometer.

For the matrix fracture toughness tests, prismatic mortar specimens (without PVA fiber) with the same dimensions used in flexural strength tests were utilized. The standards do not specify a measure of stress intensity factor of cementing materials. However, the method stated by ASTM E399: Linear-Elastic Plane-Strain Fracture Toughness K_{IC} of Metallic Materials was found to be applicable to the cement matrix [22, 23] and was therefore used throughout the study. Matrix specimens were kept in plastic bags at

95 ± 5 % RH, 23 ± 2 °C and toughness tests were performed at the end of 7 and 28 days by using four beams on each date. During the tests, three-point bending loading was applied at the rate of 0.002 mm/s over a purposely grooved 30 mm notch on the specimens as prescribed by the specification. Matrix fracture toughness values of the specimens were calculated with the equation below [23]:

$$K_Q = \frac{P_Q S}{BW^{\frac{3}{2}}} f\left(\frac{a}{w}\right),$$

where P_Q is the applied load, S the span width, B the height of the specimen, W the depth of the specimen, $f\left(\frac{a}{w}\right)$ is the Geometric calibration factor (between 1.9 and 2.2)

Linear prismatic molds, also called as shrinkage drains, were used while taking autogenous shrinkage measurements (Fig. 1). The drains were composed of inner and outer molds. The inner mold, which was embedded inside the outer mold, measured 1,000 × 60 × 90 mm. In order to prevent friction inside the inner mold, the surfaces were covered with Teflon sheets. The drains had two ends, one of which was closed and the other was free to move with an attached LVDT to measure instantaneous length changes in time. In addition to the LVDT, each drain had its own supplementary thermocouple placed between the inner and outer molds to measure temperature changes. Before placing fresh mixtures inside the drains, aerosol Teflon was sprayed over the Teflon cover and the inner mold of the drains was

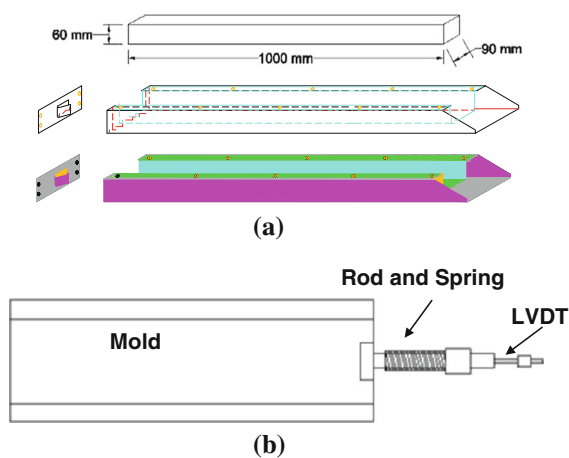


Fig. 1 Autogenous shrinkage test set-up. **a** Inner and outer molds of shrinkage drain, **b** set-up for length measurements with LVDT

completely covered with stretch wrap. This was done so mixtures were entirely isolated from the environment to better investigate the sole influence of hydration processes on autogenous shrinkage of HES-ECCs. Once the placement of fresh mixtures was completed, the top surface of the drains was covered with previously placed stretch wrap and an additional Teflon sheet. LVDT measurements were started after the final setting time of the mixtures was reached; until this time only temperature changes were recorded. Since it is not always easy to estimate the time needed for different mixtures with fiber to set, a common time interval was used for all mixtures. The time needed for LVDT measurements to begin was based on the period in which maximum heat liberation was observed for each mixture, which worked out to around 2 h for all mixtures. All of the drains were kept in laboratory conditions at 23 ± 2 °C, and 50 ± 5 % RH. The changes in LVDT and temperature measurements were recorded by a data acquisition system every 10 min for 1 week.

4 Results and discussions

4.1 Mechanical properties of HES-ECC mixtures

4.1.1 Fracture toughness

Toughness tests were conducted on prismatic mortar specimens at the ages of 7 and 28 days; the results are shown in Table 3. Each piece of data displayed in Table 3 was found by averaging the results of at least five specimens. As seen from the table, HES-ECC_2 specimens exhibited the highest toughness results with values ranging between 0.96 and 0.73 MPa × m^{1/2} at the end of 7 days. The same trend was also observed for the results obtained at the end of 28 days. In addition, HES-ECC_3 specimens resulted in the lowest results at the end of any specified time. When the fracture toughness test results of matrices (ECC without PVA fiber) are carefully evaluated, a close relationship between toughness and compressive strength is evident, since both parameters are markedly affected by the changes occurring in matrix maturity with time. The addition of saturated LWA was expected to increase the toughness results, since it was believed that internally available water inside the LWAs would trigger further hydration reactions at a

Table 3 Mechanical properties of HES-ECC mixtures

Mixture ID	Compressive strength (MPa)				Flexural strength (MPa)				Mid-span beam deflection (mm)				Fracture toughness (MPa × m ^{1/2})	
	6 h	24 h	7 day	28 day	6 h	24 h	7 day	28 day	6 h	24 h	7 day	28 day	7 day	28 day
HES-ECC_1														
Control	26.9	64.4	85.0	95.1	8.0	9.5	10.9	11.1	3.6	2.7	1.4	1.0	0.93	1.03
C_25 %	23.3	52.8	73.9	80.7	8.0	9.1	10.6	11.7	3.4	3.0	2.7	2.4	0.79	0.88
C_50 %	20.7	41.9	68.6	76.0	7.8	9.0	10.1	11.0	3.4	2.9	2.5	2.3	0.65	0.72
F_25 %	26.2	58.6	81.5	88.0	8.1	9.5	10.8	11.4	3.8	3.2	2.5	2.3	0.81	0.90
F_50 %	22.0	47.2	73.9	82.5	7.9	8.9	10.1	11.3	3.7	3.3	2.6	2.4	0.68	0.75
HES-ECC_2														
Control	33.6	68.4	84.8	93.0	8.7	10.0	11.0	12.5	2.8	2.0	1.4	1.2	0.96	1.10
C_25 %	29.7	60.8	76.5	84.0	8.6	9.6	11.0	12.2	3.1	2.4	2.2	1.9	0.82	0.90
C_50 %	27.9	44.8	62.8	74.3	7.4	9.1	10.2	11.3	2.9	2.5	2.3	2.0	0.73	0.81
F_25 %	32.0	62.3	78.6	90.0	8.8	9.7	10.3	11.9	3.5	2.9	2.2	2.2	0.84	0.90
F_50 %	28.3	51.3	67.7	78.4	7.8	9.1	9.5	11.5	3.7	3.1	2.4	2.2	0.77	0.85
HES-ECC_3														
Control	29.6	56.2	64.6	75.7	7.2	8.6	10.0	10.2	2.3	1.9	1.2	1.0	0.89	0.93
C_25 %	25.2	38.8	52.7	59.6	6.7	8.3	9.1	10.0	2.4	2.0	1.6	1.5	0.75	0.81
C_50 %	17.0	34.3	42.6	47.4	6.0	6.2	8.9	9.3	2.3	2.3	2.2	1.5	0.62	0.71
F_25 %	27.6	43.9	54.9	63.2	6.9	8.2	9.6	9.8	2.9	2.5	2.4	2.0	0.76	0.85
F_50 %	19.0	36.5	47.1	51.2	6.2	6.9	8.6	9.5	3.4	2.9	2.4	2.2	0.66	0.73

very low W/CM ratio, leading to enhanced matrix maturity and matrix fracture toughness results. However, as also seen from Table 3, the overall toughness results differ from the expectation since LWA replacement resulted in a 15–30 % reduction in toughness values of 7-day cured HES-ECC specimens. This drop is most probably due to the higher porosity of matrices with the inclusion of LWAs, since expanded perlite is much weaker and coarser than the silica sand it replaces.

It is well known that when concrete is loaded, cracks prefer to propagate along the weaker zone or big pores in the matrix [24, 25]. As the crack meets LWA particle, it can easily propagate through the weaker LWA. For ECC mixtures incorporating pre-soaked LWA, the LWA was weaker than the rest of the matrix. Cracks, therefore, prefer to propagate easily through the aggregate particles. Therefore, when LWA volume increases, higher number of weak LWA particles are available in the path of crack, resulting in smoother cracking path and less energy needed for cracking, and then lower values of fracture toughness. Since higher matrix toughness could be detrimental to achieving the desired mechanical

properties, and reducing the tendency to develop multiple-cracking [22], the use of LWA in ECC production should be helpful for achieving strain-hardening behavior.

4.1.2 Compressive strength

The compressive strength test results obtained from HES-ECC mixtures are presented in Table 3. Each piece of data given in the table is the average of six cubic specimens. As shown in Table 3, at the end of 6 h, HES-ECC_2 control specimens had the highest compressive strength value with 33.6 MPa. In the HES-ECC_1 and HES-ECC_3 specimens, these values were 26.9 and 29.6 MPa, respectively. The results showed an increasing trend up to 28 days, regardless of mixture type. An increase in compressive strength results was less after 24 h; however, this is expected since hydration reactions slowdown significantly after this time. When the results obtained from the HES-ECC_1 and HES-ECC_2 mixtures are compared, the effect of S/PC ratio on compressive strength at the end of 6 h can be seen more clearly. At the same W/CM ratio, as S/PC ratio decreased from 0.84 to 0.60, an

almost 25 % increase in the compressive strength of control specimens was monitored. The main reason for this behavior is the higher amount of high early strength PC. Another reason for increased compressive strength with lower S/PC ratio could be the finer particle size of CEM I 52.5R PC ($460 \text{ m}^2/\text{kg}$) compared to slag ($425 \text{ m}^2/\text{kg}$). In addition to the positive effect of chemical reactivity, when the number of finer particles in the mixtures increased, the pores in the cementitious matrix filled better, leading to denser microstructure and higher compressive strength results. Along with the filler effect, the higher fineness and particle surface area of PC provide more nucleating sites and OH^- ions as well as alkalis into the pore fluid [26]. When 6-h compressive strength results of HES-ECC_2 and HES-ECC_3 mixtures are compared, it can be concluded that W/CM is a better criterion in defining the changes in compressive strength. Despite the significant drop in S/PC ratio (from 0.60 to 0.00), an increase in W/CM ratio from 0.23 to 0.34 caused almost 12 % of the overall decrease in the results.

Specimens with LWA can produce higher strength due to internal curing and enhanced hydration considerations [27]; however, the strength of porous aggregates is an important factor that affects the strength of concrete [28]. Lightweight perlite aggregate is much weaker than the silica sand it replaces, and as seen in Table 3, an increase in the LWA amount caused a significant decrease in compressive strength, irrespective of replacement level. For example, replacement with 25 % coarse LWA caused a 14 % decrease in 6-h compressive strength value of HES-ECC_1 mixture. At a 50 % replacement level, the loss increased to 23 %. However, the decreasing trend was less pronounced in the case of fine LWA replacement levels; a 3 and 20 % decrease was monitored with 25 and 50 % fine LWA replacement, respectively. During the production of ECC, it is desirable to work with finer aggregates, since uniform distribution of fibers is vital for superior material characteristics. With coarser LWA usage, the formation of fiber bundles—which behave as voids in the cementitious matrix—occurs more easily. The reason for reduced compressive strength results with the addition of LWA may therefore be related to non-uniform fiber distribution and balling of fibers. It can also be correlated with the increase in stress concentrations over coarse aggregates upon loading, since the larger the aggregate size,

the higher the local water-cement ratio in the interfacial transition zone and, consequently, the weaker the concrete [24]. Despite variations observed in the results, the minimum compressive strength limit (20 MPa) set throughout the study was satisfied by all mixtures at the end of 6 h, excluding those obtained from HES-ECC_3 specimens at 50 % pre-soaked LWA replacement level.

4.1.3 Flexural strength (modulus of rupture—MOR)

Table 3 tabulates the flexural strength test results of different HES-ECC mixtures. Each piece of data presented in the table was calculated by taking the average of six prismatic specimens. As seen in the table, when the flexural strengths of control specimens at 6 h are compared, HES-ECC_2 control specimens (without pre-soaked LWA) showed the highest flexural strength attainment with 8.7 MPa. The HES-ECC_2 mixture was followed by HES-ECC_1 and HES-ECC_3 control mixtures with 8.0 and 7.2 MPa, respectively. The increase in MOR values with time was not as drastic as it was in the compressive strength results; HES-ECC_1, HES-ECC_2 and HES-ECC_3 mixtures achieved only 3.1, 3.8 and 3.1 MPa of enhancement between 6 h and 28 days of age, respectively. Although W/CM and S/PC ratios are two important parameters in realizing flexural strength development, relatively low increments in flexural strength results were observed with time compared to compressive strength. This trend can be attributed to more complex material properties that can significantly affect MOR values such as tensile strain capacity, tensile first cracking strength, and ultimate tensile strength [29]. Incorporation of LWA by 25 %, resulted in similar MOR values with control mixtures at any specified age. However, when 50 % LWA is incorporated, the MOR values were generally slightly lower than those of the control mixtures. For example, in the case of HES-ECC_3 control specimens, while the average MOR value was found to be 7.2 MPa at the end of 6 h, it dropped to 6.2 MPa with 50 % fine LWA replacement. The effect of LWA incorporation was more pronounced with coarse LWA usage; with the inclusion of 50 % of coarse LWA, MOR values decreased to 6.0 MPa. The reduced strengths with high LWA replacement level may be due to the lower strength of LWA and non-uniform distribution of fibers. The addition of significantly coarser LWA



(compared with silica sand) encourages the balling of fibers. Due to inadequate coating of fibers by the matrix, fiber-to-matrix bonding is reduced, which in turn causes decreased flexural load carrying capacity. According to NJDOT, the minimum flexural strength of fast track concrete for repair purposes should be 2.4 MPa in 6 h [18]. The California State Department of Transportation (Caltrans) requires 2.8 MPa of flexural strength attainment in 4 h before putting the pavement repair into service [30]. It therefore appears that despite the decreases in MOR results with the addition of LWA, the lowest value obtained from all HES-ECC mixtures (HES-ECC_3 with 50 % of coarse LWA replacement, 6.0 MPa) was more than enough to satisfy the minimum requirements of different authorities for a repair material.

4.1.4 Mid-span beam deflection capacity

Mid-span beam deflection values, which indirectly reflect HES-ECC ductility, are presented in Table 3. As seen from the table, results varied significantly depending on mixture proportion, LWA replacement and curing time. When the deflection values of HES-ECC_1 and HES-ECC_2 mixtures are considered, specimens with lower S/PC ratio (HES-ECC_2 mixtures) at the same W/CM ratio exhibited lower deflection values in general. According to the micro-mechanical model of steady state cracking, which is essential for achieving strain hardening behavior, high matrix fracture toughness reduces the margin to obtain multiple microcracking behavior [22]. The decreased deflection values in the HES-ECC_2 specimens compared with the other mixtures could be due to higher fracture toughness, bond strength and friction between the HES-ECC_2 matrix and the fibers (please see Fracture Toughness section). The overall deflection results of all mixtures show that the lowest values were obtained from the mixture with the highest W/CM ratio (HES-ECC_3). This finding is not in agreement with Yang et al. [31], who studied the effects of W/CM ratios ranging from 0.25 to 0.37 on the properties of ECC and concluded that the higher the W/CM ratio, the higher the flexural deflection capacity. The reason behind this behavior becomes clear in Table 1. Despite the significant increase in W/CM ratio, there was no slag incorporated in the HES-ECC_3 mixtures. This led to higher amounts of cement content but also caused a substantial increase in the amount of sand,

which is notably coarser than slag. Therefore, it is likely that the uniform distribution of fibers was interrupted due to coarser aggregate gradation in the HES-ECC_3 mixture, leading to insufficient coating of individual fibers by matrix, and thus a reduction in bonding between fiber and matrix, which is an important factor influencing ductility [32]. As shown in Table 3, as curing time was extended, a decreasing trend in deflection values of the mixtures occurred regardless of LWA usage. For example, while the average deflection value of the HES-ECC_1 control mixture at the end of 6 h was 3.6 mm, this value decreased to 2.7, 1.4 and 1.0 mm at the end of 24 h, 7 and 28 days, respectively. Reduction in mid-span beam deflection values with time is highly attributable to the continuous evolution of matrix and fiber/matrix interface properties and is expected to be limited as the matrix maturity is stabilized. The usage of saturated LWA increased the mid-span beam deflection results. For instance, at the end of 28 days, HES-ECC_1 control specimens showed a deflection value of 1.0 mm while inclusion of 25 and 50 % saturated coarse LWA increased it to 2.4 and 2.3 mm, respectively. This example also illustrates the fact that 25 and 50 % replacement with LWA yielded similar results for a given aggregate type and for a given age. Replacement of saturated fine LWA was also found to be as effective on deflection results as coarse LWA; 1.0 mm deflection value increased to 2.3 and 2.4 mm as replacement rates reached 25 and 50 % levels. The ductility of ECC material is dependent not only on fiber effectiveness in transferring stress back into the matrix, but also on the toughness of the matrix itself [8]. Therefore, the increase in deflection results with LWA replacement may be better understood by taking toughness results into consideration. Table 3 shows that toughness is reduced with the incorporation of saturated LWA, which means that the occurrence of multiple micro-cracks instead of localized cracks with larger crack widths was triggered in favor of attaining large deformability.

4.1.5 Uniaxial tensile performance

Table 4 displays uniaxial tensile behavior of HES-ECC mixtures at 7 and 28 days. Typical stress–strain curves of HES-ECC mixtures at 28 days are presented in Fig. 2. To facilitate the comparison between test results for different HES-ECC mixtures, the same



Table 4 Uniaxial tensile properties of HES-ECC mixtures

Mixture ID	Tensile strain (%)		Tensile strength (MPa)		Residual crack width (μm) 28 day
	7 day	28 day	7 day	28 day	
HES-ECC_1					
Control	1.72	1.66	4.62	5.18	~95
C_25 %	2.18	2.09	4.59	4.91	~84
C_50 %	2.22	2.19	4.46	4.78	~81
F_25 %	2.03	1.94	4.78	5.05	~89
F_50 %	2.36	2.23	4.51	4.91	~78
HES-ECC_2					
Control	1.66	1.53	5.07	5.25	~105
C_25 %	1.98	1.91	5.03	5.17	~97
C_50 %	2.12	2.08	4.67	4.93	~94
F_25 %	1.97	2.11	4.58	5.07	~95
F_50 %	2.16	2.07	4.23	4.94	~85
HES-ECC_3					
Control	1.53	1.33	4.64	4.71	~110
C_25 %	1.87	1.66	4.32	4.64	~105
C_50 %	1.98	1.71	4.17	4.43	~93
F_25 %	2.03	1.90	4.24	4.56	~94
F_50 %	2.01	1.94	3.98	4.39	~85

scales for both axes have been used for the graphs. Each result in Table 4 is an average of five to seven specimens.

As seen in Fig. 2, all HES-ECC mixtures developed in this study show strain-hardening behavior with the development of multiple cracks. In all tested HES-ECC specimens, after the first cracking, the uniaxial tensile load continues to rise accompanied by multiple cracking with strain capacities from 1.33 to 2.23 % at 28 days, which are in the range of 133–223 times the ductility of conventional concrete and normal fiber reinforced concrete. As in the measured mid-span beam deflection capacities of HES-ECC mixtures, the strain capacity measured at 28 days is slightly lower than the 7-day strain capacity for all HES-ECC mixtures. For the similar mixture proportion, the use of saturated LWA improves the tensile strain capacity of HES-ECC mixtures. Moreover, the increase in the replacement rate of LWA in HES-ECC further increases tensile ductility. As in the case of flexural strength test results, the LWA size has only a minor effect on the tensile strain capacities of HES-ECC mixtures. The improvement in the tensile strain with the use and increase in the saturated LWA content can be attributed to the fact that

the use and increase in the saturated LWA content tends to reduce matrix toughness.

Table 4 also shows that the uniaxial tensile strength of HES-ECC mixtures at 28 days of age varies from 4.39 to 5.25 MPa, depending on the mixture proportion and saturated LWA replacement levels. The tensile strength of the HES-ECC mixtures with pre-soaked LWA are slightly lower than that of the control HES-ECC mixtures without LWA. Moreover, regardless of LWA size, as the amounts of pre-soaked LWA used in the HES-ECC mixtures increase from 25 to 50 %, the uniaxial tensile strengths decrease further. For example, the uniaxial tensile strength HES-ECC specimens with saturated coarse or fine LWA replacement rate of 50 % are about 93 % that of the control HES-ECC mixtures without saturated LWA. The possible reason for this negative effect of saturated LWA has already been discussed in section of “Flexural strength (modulus of rupture—MOR)”.

Table 4 also summarizes the effect of mixture proportion and saturated LWA replacement level on the residual crack width of HES-ECC mixtures. After unloading, multiple microcracks with a small average crack width and fine crack spacing were observed. It was also found that crack width reduces slightly with the substitution of silica sand by the pre-soaked LWA. Crack width control is of primary importance for many reinforced concrete applications, since there is a close relationship between the mean or maximum crack widths and the durability of the structure. Moreover, the lower magnitude of crack width is expected to promote self-healing behavior, and thus the transport properties in cracked composites.

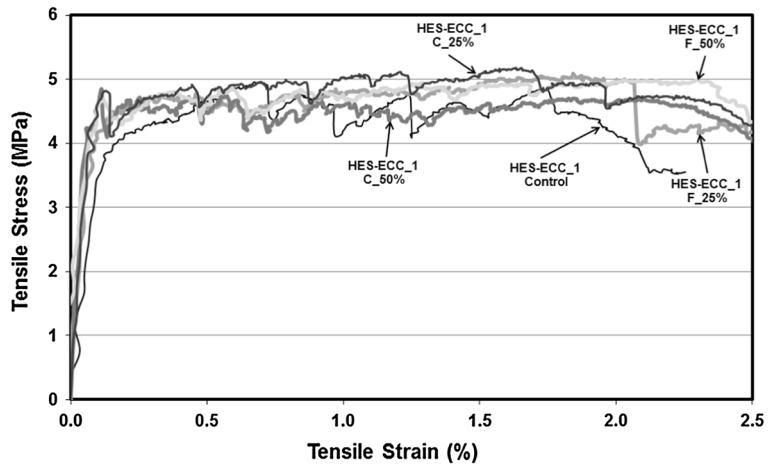
4.2 Dimensional stability of HES-ECC mixtures

4.2.1 Autogenous shrinkage

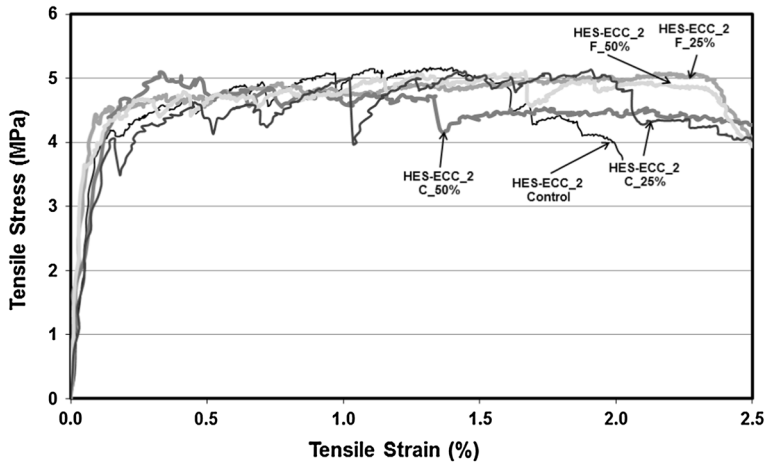
Concretes with very low W/CM ratio suffer from increased autogenous shrinkage, which is caused by self-desiccation of the cementitious matrix. As previously mentioned, the primary goal during the production of the HES-ECC mixtures was the attainment of adequate compressive strength, especially at early ages, which could substantially contribute to the faster consumption of readily available mix water. Thus, autogenous shrinkage caused by self-desiccation of the matrix must be controlled. According to reports, conventional curing procedures are not sufficient to



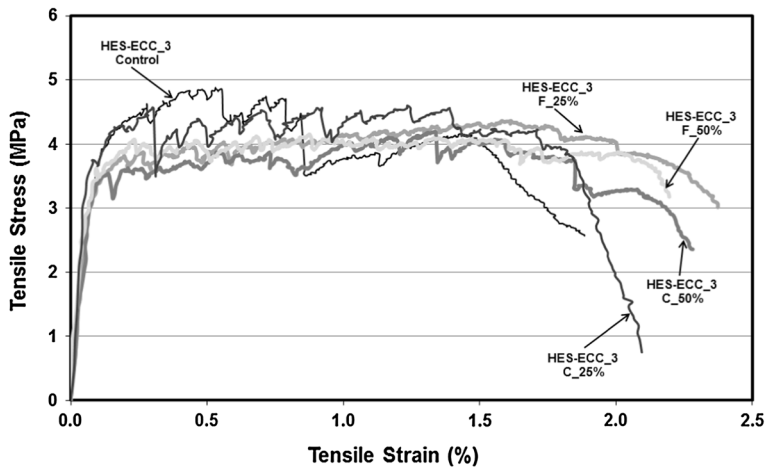
Fig. 2 Typical tensile stress–tensile strain curves of HES-ECC mixtures at age of 28 days



(a) HES-ECC_1

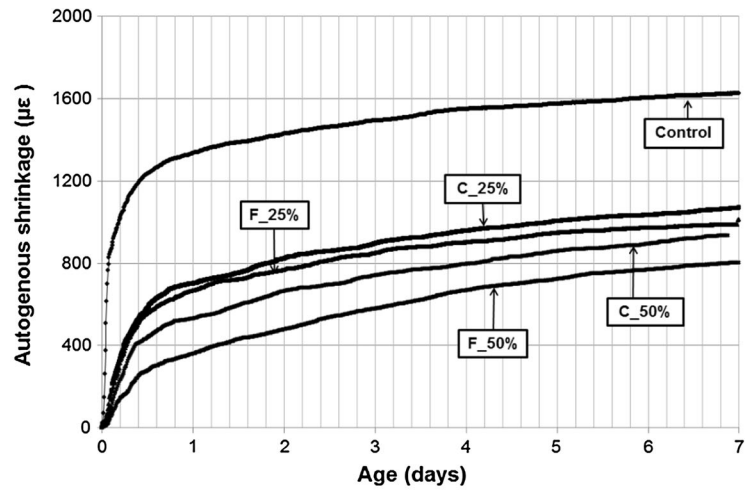


(b) HES-ECC_2

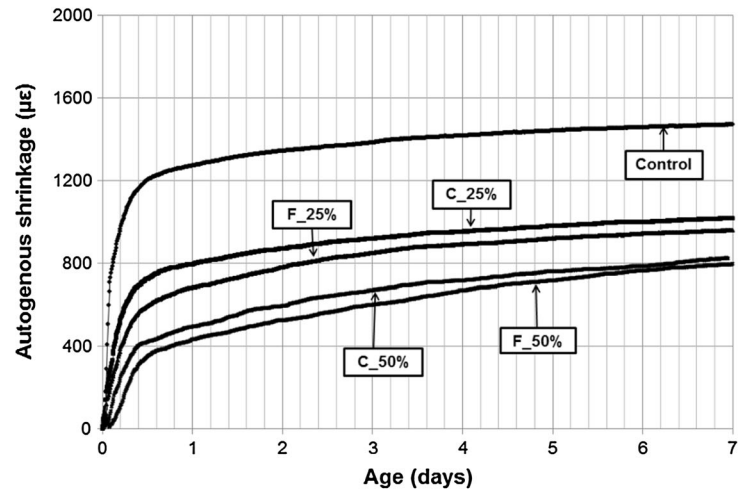


(c) HES-ECC_3

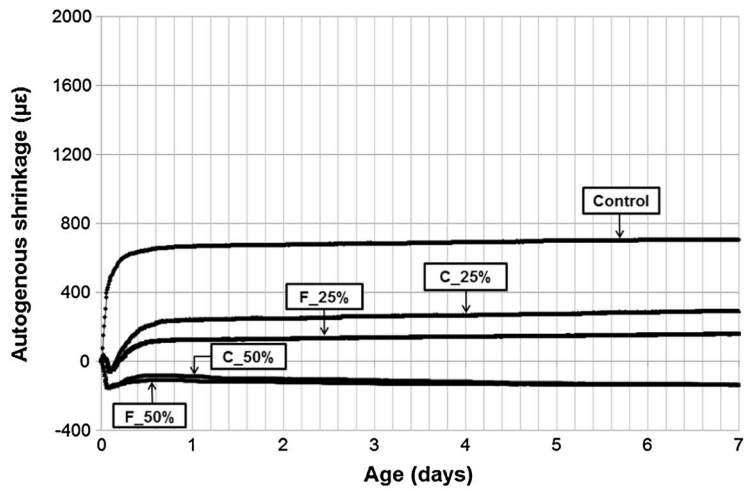
Fig. 3 Autogenous shrinkage of HES-ECC mixtures



(a) HES-ECC_1



(b) HES-ECC_2



(c) HES-ECC_3



eliminate autogenous shrinkage in concrete due to the restrictions of matrix tightness on the water transportation [33]. For this reason, the production of HES-ECC mixtures involved a proven technique to minimize autogenous shrinkage strains where pre-soaked LWAs are used as internal curing agents.

Figure 3 shows autogenous shrinkage of HES-ECC mixtures measured from 2 h after mixing up to 1 week as a function of age. As seen from the figure, all mixtures except HES-ECC_3 mixtures with LWA show an increase in the results with time, regardless of mixture type. This trend, which is directly related to the acceleration of hydration reactions and self-desiccation of the cementitious matrix, was found to be quite reasonable. It is also important to note that for all mixtures, most of the autogenous shrinkage strains were developed until the end of 1 day after final setting time. This observation, therefore, suggests that the prevention of excessive self-desiccation and autogenous shrinkage cracking in HES-ECC structures should involve techniques that are effective for at least 1 day after final setting time.

As evident from Fig. 3, the highest autogenous shrinkage development at the end of 7 days was exhibited by the HES-ECC_1 control mixture with $1,627 \mu\epsilon$. This value decreased to $1,471$ and $706 \mu\epsilon$ for HES-ECC_2 and HES-ECC_3, respectively. The changes in the results were not drastic and started to stabilize beyond 1 day as the hydration reactions start to slow down. In the HES-ECC_3 control mixture, the lower autogenous shrinkage values were found to be closely related to the higher W/CM ratio, which is in good correlation with the literature [34–37]. Since autogenous shrinkage is the result of water consumption due to cement hydration, the greater free water content results in less autogenous shrinkage. The lower autogenous shrinkage of the HES-ECC_3 control specimens can also be attributed to the substantial decrease in cementitious materials content (cement+slag) and the increase in aggregate content, both of which significantly affect hydration reactions, restraint effect and self-desiccation (see Table 1).

The addition of pre-soaked LWAs into HES-ECC mixtures caused significant changes in autogenous shrinkage results. For example, replacement with 25 % coarse LWA caused a 34 % decrease in autogenous shrinkage of the HES-ECC_1 control specimens. This value increased to 38 % with fine LWA usage. As the pre-soaked LWA replacement level was increased to

50 %, the decreasing trend became even more evident, with 43 and 51 % reductions observed for coarse and fine LWAs, respectively. The same trend was monitored for the rest of the mixtures as well. Specimens with fine LWAs may show higher reduction in autogenous shrinkage results due to more uniform distribution of the aggregates in the cementitious matrix. The effectiveness of internal curing through pre-soaked LWA usage is significantly affected by the particle size and water absorption capacity of the aggregate used. It has been reported that the small particle size and coarse pore structure of LWA achieve optimum internal curing [38]. Therefore, the explanation for lower autogenous shrinkage results with fine LWA could be that the spacing among the LWAs was reduced due to better distribution of finer particles, making paste volume more accessible to the water in the internal reservoirs. It is important to note that in order to prevent self-desiccation of the matrix, the diffusion of water from the LWAs into the matrix must be as fast as possible, since the transportation of water slows as the paste gets impermeable with further hydration. Although coarse LWAs can absorb more water (144 %) compared to fine LWAs (131 %), the results are surprising in that HES-ECC specimens with coarse LWAs showed higher autogenous shrinkage strains after 7 days. This discrepancy indicates that it is not the total water amount retained in LWA pores that is the best parameter of internal curing efficiency, but the fact that the water is effectively used to neutralize self-desiccation.

The effectiveness of pre-soaked LWAs in mitigating autogenous shrinkage can be best detected by checking the autogenous strain development in the HES-ECC_3 mixture. When the data presented in Fig. 3 were evaluated, it was clear that LWA replacement, regardless of size and quantity, was much more efficient for HES-ECC_3 than for other mixtures. Figure 3 also shows that the addition of 25 % coarse and fine LWA into the mixtures substantially minimized strain development due to self-desiccation, so that autogenous strain developments after 7 days were only 293 and $159 \mu\epsilon$ for coarse and fine LWA additions, respectively. It is also clear from Fig. 3 that for a very limited time, the curves of these specimens went down to the negative portion of the graph, implying swelling of the pastes, which is also frequently reported in the literature [39]. Expansion observed in the HES-ECC_3 specimens incorporating

50 % coarse and fine LWA correspond the above-mentioned trend, with -155 and $-159 \mu\epsilon$, respectively. One must note that this behavior of the HES-ECC_3 mixtures with 50 % LWA is one of most important criteria for obtaining truly resilient repair materials; it may lead to the realization of totally crack-free materials because of negative autogenous shrinkage capacity with the characteristics of high early strength and high deformability.

5 Conclusions

In this study, composites incorporating high volumes of slag with the characteristics of high early strength, high deformability and superior dimensional stability were developed. HES-ECC mixtures with two different W/CM (0.23 and 0.34) and S/PC (0.60 and 0.84) were produced. During the production, coarse (with MAS of 4 mm) and fine (with MAS of 2 mm) pre-soaked LWAs were substituted with silica sand at fractions of 25 and 50 % by volume in order to take advantage of the dual efficiency of LWAs on ductility and early age cracking. Control specimens with no LWA replacement were also produced for comparison purposes. Mechanical properties and autogenous shrinkage properties of HES-ECC mixtures were investigated, and the following results were drawn:

1. Although the compressive strength results were strongly influenced by the changes in W/CM, S/PC and pre-soaked LWA incorporation levels, the HES-ECC mixtures produced in this study (with the exception of HES-ECC_3 specimens with 50 % of LWA replacements) satisfy the minimum compressive strength value of 20 MPa in 6 h. The minimum flexural strength value obtained from the mixtures was found to be 6 MPa or higher at the end of 6 h, which is far beyond from the minimum values set by different authorities [19, 30]. These results show that the repair materials made with the HES-ECC mixtures designed in this study can effectively be returned to service in 6 h or less without compromising strength requirements
2. The minimum flexural deflection capacity was obtained from the HES-ECC control specimens

with 2.3 mm in 6 h. This increased ductility under bending is strongly related to reduction in matrix toughness and the effectiveness of fibers in transferring stresses. The superior ductility of HES-ECC specimens upon bending and uniaxial tension is an indispensable material property in the realization of durable repairs

3. Although some of the mixtures have triggered increments in autogenous shrinkage strains (especially control specimens), addition of pre-soaked LWAs effectively minimized self-desiccation. Moreover, autogenous shrinkage results of the HES-ECC_3 mixtures with 50 % pre-soaked LWAs show that with proper adjustments, concrete repairs that are truly resistant to cracks occurring due to self-desiccation can be produced with sufficient mechanical properties

Acknowledgments The authors gratefully acknowledge the financial assistance of the Scientific and Technical Research Council (TUBITAK) of Turkey provided under Project: MAG-112M035, Turkish Academy of Sciences, Young Scientist Award program and Feyzi AKKAYA Scientific Activates Supporting Fund (FABED) Young Investigator Research Award.

References

1. Frangopol DM, Furuta H (2000) In: Proceedings of the US–Japan workshop on life-cycle cost analysis and design of civil infrastructure systems, Honolulu, Hawaii
2. Narayan W (2007) Infrastructure, climate change, sustainability: the challenge of design-strength or durability. *Concrete* 41(9):31–33
3. Mays G (1992) Durability of concrete structures: investigation, repair, protection. E & FN Spon, London
4. AASHTO PP 1-5 (2002) “The bottom line” American Association of State Highway and Transportation Officials, Washington, DC
5. Li VC (2005) Engineered cementitious composites. In: Proceedings of ConMat’05, Vancouver, Canada, CD-documents/1-05/SS-GF-01_FP.pdf
6. Mather B, Warner J (2004) Why do concrete repairs fail, interview held at University of Wisconsin, Department of Engineering Professional Development, Wis. http://epdweb.engr.wisc.edu/AEC_Articles/07_Concrete_Repair_text.html
7. Whiting D, Nagi M (1994) Strength and durability of rapid highway repair concretes. *Concr Int* 16(9):36–41
8. Li VC (1997) Engineered cementitious composites tailored composites through micromechanical modeling. In: Banthia NA, Bentur, Mufti A (eds) Fiber reinforced concrete: present and the future. Canadian Society for Civil Engineering, Montreal, pp 64–97



9. Li VC (2003) On engineered cementitious composites (ECC): a review of the material and its applications. *Adv Concr Technol* 1:215–230
10. Lin Z, Li VC (1997) Crack bridging in fiber reinforced cementitious composites with slip-hardening interfaces. *Mech Phys Solids* 45:763–787
11. Lin Z, Kanda T, Li VC (1999) On interface property characterization and performance of fiber reinforced cementitious composites. *Concr Sci Eng* 1:173–184
12. Wang S, Li VC (2006) High early strength engineered cementitious composites. *ACI Mater J* 103(2):97–105
13. Seehra SS, Gupta S, Kumar S (1993) Rapid setting magnesium phosphate cement for quick repair of concrete pavements—characterization and durability aspects. *Cem Concr Res* 23(2):254–266
14. Knofel D, Wang JF (1994) Properties of three newly developed quick cements. *Cem Concr Res* 24(5):801–812
15. Sprinkel MM (1998) Very-early-strength latex-modified concrete overlay, Report No. VTRC99-TAR3, Virginia Department of Transportation, Richmond, Virginia
16. Li M, Li VC (2011) High-early-strength engineered cementitious composites for fast, durable concrete repair—material properties. *ACI Mater J* 108(1):3
17. Parker F, Shoemaker ML (1991) PCC pavement patching materials and procedures. *Mater Civil Eng* 3(1):29–47
18. Kurtz S, Balaguru P, Consolazio G, Maher A (1997) Fast track concrete for construction repair, Report No. FHWA 2001-015, New Jersey Department of Transportation, Trenton, NJ
19. Federal Highway Administration (FHWA), Manual of Practice (1999) Materials and procedures for rapid repair of partial-depth spalls in concrete pavements
20. Şahmaran M, Yucel HE, Demirhan S, Arik MT, Li VC (2012) Combined effect of aggregate and mineral admixtures on the tensile ductility of ECC. *ACI Mater J* 109(6):627–638
21. Li VC, Li C, Wu S, Wang S, Ogawa T (2002) Interface tailoring for strain-hardening PVA-ECC. *ACI Mater J* 99(5):463–472
22. Li VC, Mishra DK, Wu HC (1995) Matrix design for pseudo strain-hardening fiber reinforced cementitious composites. *RILEM J Mater Struct* 28(183):586–595
23. ASTM Standard E399. (2003). Test method for plane-strain fracture toughness of metallic materials. West Conshohocken
24. Mehta PK, Monteiro PJM (2006) Concrete: structure, properties, and materials, 3rd edn. McGraw Hill, New York
25. Qian S, Li VC (2007) Simplified inverse method for determining the tensile strain capacity of strain hardening cementitious composites. *Adv Concr Technol* 5:235–246
26. Li G, Zhao X (2003) Properties of concrete incorporating fly ash and ground granulated blast-furnace slag. *Cement Concr Compos* 25:293–299
27. Lura P, Bentz DP, Lange DA, Kovler K, Bentur A (2004) Pumice aggregates for internal water curing, In: PRO 36: Proceedings of the international RILEM symposium on concrete science & engineering—a tribute to Arnon Bentur, RILEM Publications S.A.R.L., 137–151
28. Zhang MH, Gjorv OE (1991) Mechanical properties of high-strength lightweight concrete. *ACI Mater J* 88(3):240–247
29. Qian S, Zhou J, De Rooij MR, Schlangen E, Ye G, Van Breugel K (2009) Self-healing behavior of strain hardening cementitious composites incorporating local waste materials. *Cement Concr Compos* 31:613–621
30. Anderson J (2001) Paving repair finds a four-hour champion. *Concr Constr* 46(12):69–70
31. Yang Y, Gao X, Deng H, Yu P, Yao Y (2010) Effects of water/binder ratio on the properties of engineered cementitious composites. *Wuhan Univ Technol—Mater Sci Ed* 25(2):298–302
32. Soroushian P, Nagi M, Hsu J (1992) Optimization of the use of lightweight aggregates in carbon fiber reinforced cement. *ACI Mater J* 89:267–276
33. Bentz DP, Snyder KA (1999) Protected paste volume in concrete—extension to internal curing using saturated lightweight fine aggregate. *Cem Concr Res* 29(11):1863–1867
34. Tazawa E, Miyazawa S (1993) Autogenous shrinkage of concrete and its importance in concrete technology. In: Bazant ZP, Carol L (eds) Creep and shrinkage of concrete. Proceedings of the 5th international RILEM symposium, E & FN Spon, London, pp. 159–168
35. Brooks JJ, Cabrera JG, Megat Johari MA (1998) Factors affecting the autogenous shrinkage of silica fume high-strength concrete. In: Tazawa E (ed) Proceedings of international workshop on autogenous shrinkage of concrete. E & FN Spon, Hiroshima, Japan, pp 195–201
36. Mak SL, Ritchie D, Taylor A, Diggins R (1998) Temperature effects on early age autogenous shrinkage in high performance concretes. In: Tazawa E (ed) Proceedings of international workshop on autogenous shrinkage of concrete. E & FN Spon, Hiroshima, Japan, pp 155–165
37. Persson BSM (1998) Shrinkage of high-performance concrete. In: Tazawa E (ed) Proceedings of international workshop on autogenous shrinkage of concrete. E & FN Spon, Hiroshima, Japan, pp 105–115
38. Zhutovsky S, Kovler K, Bentur A (2002) Efficiency of lightweight aggregates for internal curing of high strength concrete to eliminate autogenous shrinkage. *Mater Struct* 35(2):97–101
39. Bentur A, Igarashi S, Kovler K (2001) Prevention of autogenous shrinkage in high strength concrete by internal curing using wet lightweight aggregates. *Cem Concr Res* 31(11):1587–1591